

Investigation of the absorption of laser radiation and the degree of compression of spherical microtargets under exploding shell conditions

S. A. Bel'kov, A. V. Bessarab, A. V. Veselov, S. G. Garanin, G. V. Dolgoleva, A. I. Zaretskiĭ, G. A. Kirillov, G. G. Kochemasov, N. V. Maslov, I. N. Nikitin, S. I. Petrov, A. V. Ryadov, A. V. Senik, N. A. Suslov, and S. A. Sukharev

(Submitted 11 October 1989)

Zh. Eksp. Teor. Fiz. **97**, 834–841 (March 1990)

An experimental investigation was made of the absorption of laser radiation (of intensity in the range 10^{14} – 10^{15} W/cm²) and generation of fast particles in the ISKRA-4 facility. Measurements were made of the degree of compression of spherical microtargets filled with gaseous DT containing a small proportion of Ne. The experimental results were compared with one-dimensional gasdynamic calculations.

One of the main tasks in research on laser thermonuclear fusion is to find the optimal conditions for irradiation of microtargets, particularly the optimal radiation intensity reaching the target. An increase in this intensity increases the coronal plasma pressure, which ensures the necessary degree of energy accumulation in the case of moderate values (~ 10 – 30) of the ratio of the target radius R_0 to the shell thickness ΔR . However, an increase in the intensity tends to change the coronal plasma to the collisionless state. The energy is then absorbed in undesirable channels: large numbers of “hot” electrons are generated and their energies are of the order of several tens of kiloelectron-volts, which results in preheating of the shell and fuel in the target; in the low-density part of the corona the hot-electron pressure creates high-energy ions and this eventually reduces the hydrodynamic efficiency.

The present paper reports the results of experimental investigations on irradiation of spherical glass microtargets with radiation from the ISKRA-4 iodine laser facility (emission wavelength $\lambda_0 = 1.315 \mu\text{m}$) at intensities in the range 10^{14} – 10^{15} W/cm² using laser pulses of ~ 0.2 – 0.4 ns duration.^{1–3} Targets with 120–240 μm diameter and aspect ratio in the range $R_0/\Delta R \approx 120$ – 30 were used. In some cases the glass shells of the targets were coated by a plastic layer of C₈H₈ which was ~ 0.5 – $3 \mu\text{m}$ thick. An experimental study under these irradiation conditions made it possible to check the theory of the mechanisms of laser radiation absorption and “fast” particle generation, as well as the theory of the dynamics of plasma expansion and compression of the DT gas, which are important topics in determination of the requirements that laser systems must satisfy and in forecasting the results which may be expected when facilities capable of higher powers are built.

1. INVESTIGATION OF LASER RADIATION ABSORPTION

One of the key topics in the problem of laser thermonuclear fusion is the efficiency and mechanisms of absorption of radiation in the plasma corona of a laser microtarget. The energy delivered to the target and its distribution between the various absorption channels depends largely on the working conditions in the target.

At laser radiation intensities $I_L \approx 10^{14}$ – 10^{15} W/cm² when the wavelength is $\lambda_0 \approx 1 \mu\text{m}$ a dilatation discontinuity should form under the influence of the ponderomotive force in the region where the plasma has the critical density ρ_c (Refs. 4 and 5). The presence of this discontinuity reduces

the bremsstrahlung absorption coefficient, but makes the resonant absorption more effective.⁶ Laser radiation is then transformed into plasma waves and the decay of the latter creates hot electrons.

The role of the resonant absorption was investigated by determination of the dependences of the absorption coefficient K_a , the energy of fast ions E_f , the temperature of hot electrons T_h , and the energy of hard x rays E_h on the intensity I_L and the angular distribution of the laser radiation incident on a target.

We determined the absorbed energy E_a using calorimeters based on pyroelectric detectors. The energy E_f transmitted to fast ions was determined by recording the spectrum of the expanding ions with the aid of ion collectors at velocities $v_i \approx (0.3$ – $6) \times 10^8$ cm/s.

The hot electron temperature T_h and the energy of hard x rays E_h were deduced from the spectrum of continuous x-ray radiation recorded using the method of K filters in the photon energy range $h\nu \approx 2$ – 80 keV (Ref. 7). The experimental value of the absorption coefficient was found from the ratio $K_a = E_a/E_L$, where E_L is the energy delivered to the interaction chamber.

The experimental results were compared with calculations carried out using an SND gasdynamic program⁸ which allowed for the absorption and energy release due to laser radiation. We used a physical mathematical model of the absorption, which had certain features in common with the model used in Ref. 9 and which allowed us to calculate—in the geometric-optics approximation—the bremsstrahlung and resonant absorption subject to a self-consistent phenomenological allowance for the increasing steepness of the density profile.^{4,5} The energy absorbed by the bremsstrahlung mechanism was converted into the thermal energy of electrons in the region where the plasma density was below the critical value. Part of the energy absorbed resonantly was ignored because only rough allowance was made for the losses due to the acceleration of fast ions. The remaining energy was transmitted to hot electrons, which were responsible for the bulk heating of the target. The ratio of these energies was calculated allowing for the corona expansion dynamics employing a self-similar model of the process of isothermal expansion of a plasma with two electron components.¹⁰ The temperature of hot electrons was determined by a scaling procedure described in Ref. 11. The known density and temperature of “hot” electrons were used to calculate the integral energy of hard x rays.

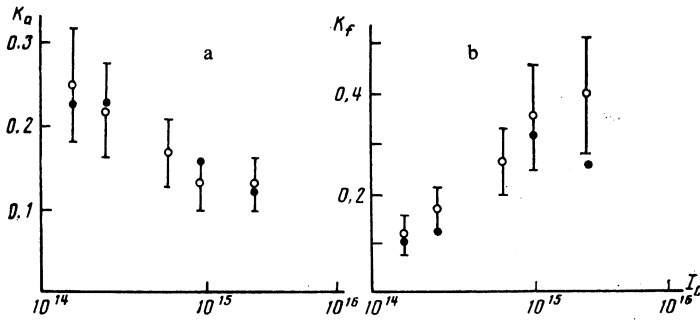


FIG. 1. Dependences of the absorption coefficient (a) and the fraction of the energy carried by fast ions (b) on the laser radiation intensity: ○) experimental results; ●) calculations.

An investigation of the dependences of the parameters K_a , E_f , and E_h^γ on the intensity I_h was made in two types of experiment. In the experiments of the first type the target parameters were constant (initial diameter $2R_0 \approx 160 \mu\text{m}$, wall thickness $\Delta R \approx 1 \mu\text{m}$) and so were the focusing conditions (with the center of the target shifted by $\Delta z \approx 100 \mu\text{m}$ relative to the minimum of the focusing spot in the direction of the subfocal region), but the energy delivered to the chamber was varied within the range $E_L \approx 20\text{--}470 \text{ J}$ and the duration of the laser pulses was also varied within $\tau_L \approx 0.16\text{--}0.4 \text{ ns}$. The experimental and calculated dependences of the absorption coefficient, and of the fraction of the energy carried by the fast ions $K_f = E_f/E_a$ on the laser radiation intensity I_L are plotted in Fig. 1.

In experiments of the second type we varied the target diameter in the range $2R_0 \approx 120\text{--}250 \mu\text{m}$, but kept the laser pulse parameters constant ($E_L \approx 400 \text{ J}$, $\tau_L \approx 0.3 \text{ ns}$). The angular characteristics of the radiation reaching the target were kept approximately constant by ensuring that the longitudinal shift Δz was such that the ratio $\Delta z/2R_0$ was approximately constant. We plotted in Fig. 2 the experimental and calculated dependences of the parameters K_a and K_f on the initial target diameter.

These two series of experiments demonstrated that a reduction in the laser radiation intensity increased, as expected, the absorption coefficient. The results obtained can

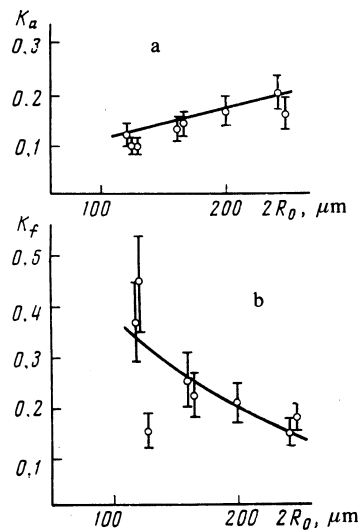


FIG. 2. Dependences of the absorption coefficient (a) and of the fraction of the energy carried by fast ions (b) on the initial target diameter: ○) experimental results; the continuous curves are calculated.

be attributed qualitatively to a reduction in the deformation (discontinuity) of the density profile and a reduction in the electron temperature T_e of the plasma when I_L is lowered. In fact, in the first approximation, the optical thickness of the plasma corona considered in terms of the bremsstrahlung absorption is proportional to $\rho_-^+ c_s \tau_L / T_e^{3/2}$, where $c_s \propto T_e^{1/2}$ is the velocity of sound and ρ_- is the density at the lower edge of the discontinuity. According to Ref. 12, we have

$$\rho_- \approx \rho_c [1 + \alpha (T_e/I_L)^{1/2}]^{-1},$$

where α is a constant. In the range of laser radiation intensities of interest to us, we have $\rho_- \propto I_L^{-0.16}$ and $T_e \propto I_L^{1/2}$, so that the optical thickness is proportional to $I_L^{-2/3} \tau_L$. At low values of the optical thickness the bremsstrahlung absorption coefficient exhibits a similar dependence. The resonant absorption coefficient K_r increases on increase in I_L because of broadening of the resonance curve.¹³ However, the rate of rise of K_r is insufficient for compensation of the reduction in the bremsstrahlung absorption coefficient K_b . It should be noted that if $\tau_L \sim 0.3 \text{ ns}$, the absolute value of K_r is less than the values of K_r found using short pulses in the range $\tau_L \leq 0.1 \text{ ns}$ (Ref. 14).

The reduction in K_r when I_L is lowered reduces the energy transferred to the hot electrons. This was confirmed by recording of the continuous x-ray radiation spectrum. For example, when the intensity was in the range $I_L \sim (1\text{--}2) \cdot 10^{15} \text{ W/cm}^2$, the hot electron temperature was $T_h \approx 12\text{--}13 \text{ keV}$ and the energy of hard x rays was $E_h^\gamma \approx (0.5\text{--}1) \times 10^{-3} \text{ J}$, whereas for intensities in the range $I_L \sim (2\text{--}3) \times 10^{14} \text{ W/cm}^2$ the signals reaching detectors of hard x rays were below the sensitivity threshold ($E_h^\gamma < 10^{-6} \text{ J}$).

An investigation of the dependences of these parameters on the angular characteristics of the focused laser radiation was made employing a target with a diameter $2R_0 \approx 160 \mu\text{m}$ when the laser pulse energy was $E_L \approx 300\text{--}400 \text{ J}$ and the duration was $\tau_L \approx 0.2\text{--}0.3 \text{ ns}$. The angular characteristics changed because of the different longitudinal shift of the target center to the subfocal region ($\Delta z = 0\text{--}250 \mu\text{m}$). It should be mentioned that focusing of radiation on a target in the ISKRA-4 facility was performed by four parabolic mirrors with a diameter $D = 27 \text{ cm}$ and a focal length $F = D$.

The dependences of the parameter K_f (Fig. 3b) and of the ratio E_h^γ/E_a (Fig. 3c) on the longitudinal shift of the target center relative to the minimum of the irradiation spot had characteristic minima at $\Delta z/2R_0 \approx 0.75$. This behavior could be due to the fact that the shifts corresponded to opti-

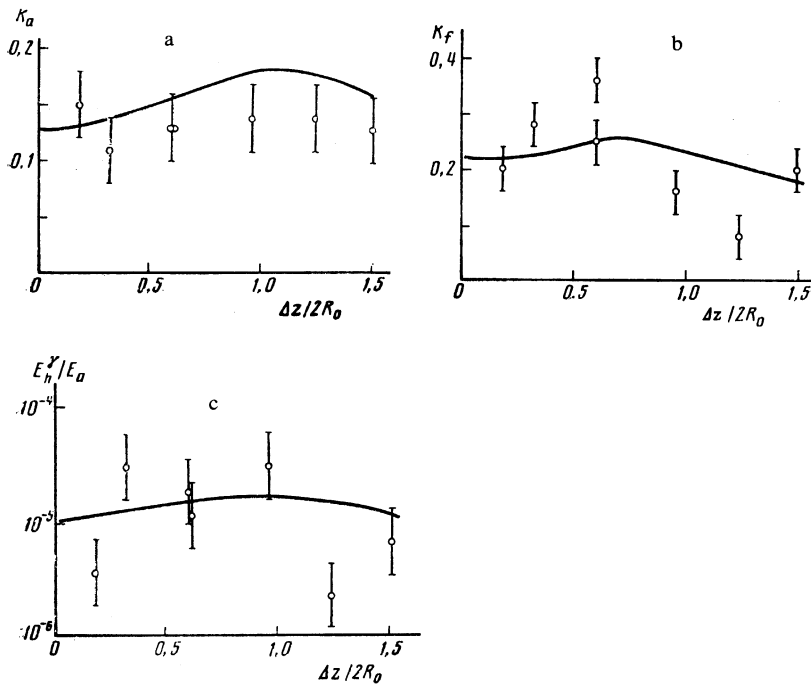


FIG. 3. Dependences of the absorption coefficient (a), the fraction of the energy carried by fast ions (b), and the energy of hard x-ray radiation (c) on the longitudinal shift of the target center relative to the minimum of the irradiated spot: \circ) experimental results; the continuous curves are calculated.

mal (from the point of view of the resonant absorption) angles of incidence of the radiation on the plasma. However, a change in the shift of the target center altered not only the angular characteristics of the laser radiation, but also the intensity I_L . This changed the balance between the resonant and bremsstrahlung absorption coefficients, and the consequence was a weak dependence of the absorption coefficient K_a on the shift (Fig. 3a).

2. INVESTIGATION OF COMPRESSION OF GLASS SHELLS

Another important problem is the stability of compression of shells and the ability to reach high gas densities. An experimental investigation of the degree of compression of spherical shells was made using the ISKRA-4 facility generating laser pulses of $E_L = 300\text{--}400$ J energy and $\tau_L = 0.2\text{--}0.35$ ns duration. The diagnostics of the volume compression δ and the final density ρ_f of the DT gas was performed in three ways:

a) by determination of the size of the image of the central part of the target recorded using x rays generated by the plasma itself and a pinhole camera (without temporal resolution but with a spatial resolution of at least $10\ \mu\text{m}$);

b) from the spatial size of the radiation representing the Ne lines, which was added to the DT gas (so that the relative partial pressure of Ne did not exceed 7%);

c) from the spectral width $\Delta\lambda_{Ly}$ of the Lyman series of lines of the hydrogen-like Ne.

The line x-ray radiation was recorded with a spectrograph capable of spatial resolution utilizing a KAP crystal.¹⁵ The spectral resolution was governed mainly by the finite dimensions of the line x-ray source and it amounted to $\Delta\lambda \approx 18$ mÅ when the size of the luminous region was about $50\ \mu\text{m}$. The spatial resolution was governed by the size of the entry slit and was at least $35\ \mu\text{m}$.

The actual construction of the channel used to record the line x-ray radiation with a spatial resolution imposed limitations on the background of continuous x-ray radiation

emitted by the target corona. The intensity of the coronal radiation was reduced by coating sometimes the glass shells with a layer of polyparaxylylene (PPX) of different thickness. This made it possible to change also, in the desired manner, the aspect ratio of the shells, which was varied in a wide range.

An investigation of the dynamics of compression of the DT gas under exploding shell conditions indicated that the main parameter governing the degree of volume compression δ was the ratio of the shell mass M_{sh} to the gas mass M_G . The experimental values of δ obtained for high-aspect shells ($R_0/\Delta R > 70$) using a pinhole camera exhibited a considerable scatter when considered as a function of the ratio M_{sh}/M_G (Fig. 4). A power-law approximation of the dependence on this parameter analyzed by the least-squares

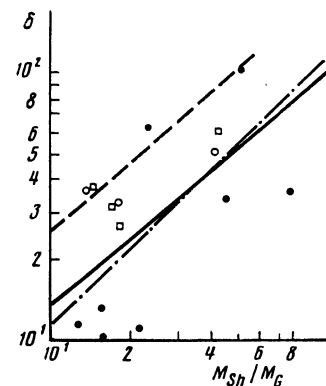


FIG. 4. Dependences of the degree of volume compression δ on the ratio of the shell mass M_{sh} to the gas mass M_G : \bullet) pinhole camera results; \circ) deduced from the width of the Ly_β line of Ne x; \square) calculated degree of compression for experiments on targets filled with a DT + Ne mixture; the continuous curve approximates the experimental points by the least-squares method; the chain line is the dependence taken from Ref. 16; the dashed line represents gasdynamic calculations carried out using the SND program.

TABLE I. Results of experiments on compression of spherical targets filled with a DT + Ne mixture and comparison with gasdynamic calculations made using the SND program.

Experiment No.	$2R_M, \mu\text{m}$	$\Delta R_{\text{SiO}_2}, \mu\text{m}$	$\Delta R_{\text{PPX}}, \mu\text{m}$	E_L, J	τ_L, ns	$\rho_0, \text{g/cm}^3$	E_a, J exp. (calc.)
1 *)	159	0.9	0.5	209	0.3	$6.5 \cdot 10^{-3}$	26 (26)
2 *)	157	0.8	2	250	0.17	$4 \cdot 10^{-3}$	23 (23)
3	156	1.0	0	370	0.2	$6.7 \cdot 10^{-3}$	34 (37)
4	122	1.7	2.1	280	0.18	$8.3 \cdot 10^{-3}$	33 (38)

Experiment No.	$\Delta \lambda_{\text{Ly}\beta}^{\text{Ne}}, \text{m}\text{\AA}$ exp. (calc.)	$\Delta \lambda_{\text{Ly}\beta}^{\text{Ne}}, \text{m}\text{\AA}$ exp. (calc.)	$\rho_f^{\text{pinhole}}, \text{g/cm}^3$	$\rho_f^{\text{pinhole}}, \text{exp. (calc.)}$	N exp. (calc.)
1 *)	50 (44)	55 ± 5 (68)	0.2	0.10 (0.21)	10^4 ($5 \cdot 10^4$)
2 *)	50 ± 10 (80)	81 ± 5 (100)	0.24	0.16 (0.20)	10^4 (10^6)
3	90 ± 20 (80)	95 ± 15 (110)	0.07	0.2 (0.26)	$4 \cdot 10^5$ ($9 \cdot 10^6$)
4	—	92 ± 10 (100) **)	0.36	0.80–1.00 (1.02)	10^4 ($4 \cdot 10^5$)

*) The experimentally absorbed energy E_a was used in the gasdynamic calculations.

***) The separation between the maxima of two components of the Ly_β line is given.

method gave

$$\delta = a \left(\frac{M_{\text{sh}}}{M_G} \right)^b, \quad (2.1)$$

where $a = 1.7$ and $b = 0.88$. These results were in reasonable agreement with those reported earlier¹⁶ for facilities using Nd and CO_2 lasers ($a = 1.15, b = 1$). The dependence of the degree of compression δ on M_{sh}/M_G obtained by numerical modeling carried out using the SND program and the experimental results obtained using the ISKRA-4 facility was in qualitative agreement with Eq. (2.1) ($b = 0.86$), but the absolute values of δ were approximately twice as large as the experimental values ($a = 3.6$).

Determination of the degree of compression using the pinhole camera gave only a rough estimate of the final density of the DT gas, so that when the resolution of this camera was $\sim 30 \mu\text{m}$ and the size of the central compressed core was $\sim 10 \mu\text{m}$, the error in the determination of the volume compression became 100%.

A more accurate determination of the degree of compression was obtained in experiments on targets filled with gaseous DT containing a small proportion of neon. The compressed gas density was determined by comparing the experimentally recorded profiles of the spectral lines of the Ne X ion lines and those calculated for a plasma with a given composition assuming different values of the density ρ and the temperature T_e .

We should mention that in this case a lower estimate of

the density of the compressed DT gas was obtained, since (according to the gasdynamic calculations) the moment of attainment of the maximum temperature in the core (and, consequently, the moment of the strongest emission of the Ne X lines) did not coincide with the moment of maximum compression.

A comparison of the results of these gasdynamic calculations carried out using the SND program with the experimental results obtained using the ISKRA-4 facility was made as follows. The values of the density and temperature T_e at the moment of maximum compression were calculated for a given absorbed energy and for a given energy of the laser radiation reaching the target; these values were then used to obtain theoretical profiles of the Ne X spectral lines. The calculated widths of the Ly_α and Ly_β lines ($\Delta \lambda_{\text{Ly}_\alpha}$ and $\Delta \lambda_{\text{Ly}_\beta}$) were then compared with the experimental widths of the corresponding lines.

Table I gives the experimental and calculated parameters of the plasma in the laser corona and in the compressed core (see also Fig. 4) obtained for targets filled with a mixture of DT and Ne. This comparison demonstrated a satisfactory agreement between the gasdynamic calculations and the experimental data.

These results led us to the conclusion that under the exploding shell conditions it was not possible to reach high densities of the DT gas in the range $\rho_f \gtrsim 1 \text{ g/cm}^3$ in the case of the high-aspect ratios characterized by $R_0/\Delta R \gtrsim 80$ (experiments 1–3 in Table I), since the preheating by hot elec-

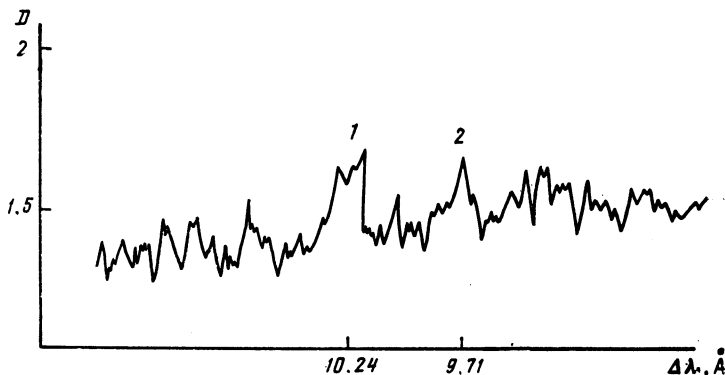


FIG. 5. Densitogram of the Ne X spectrum recorded in experiment No. 4: 1) Ly_β line; 2) Ly_γ line.

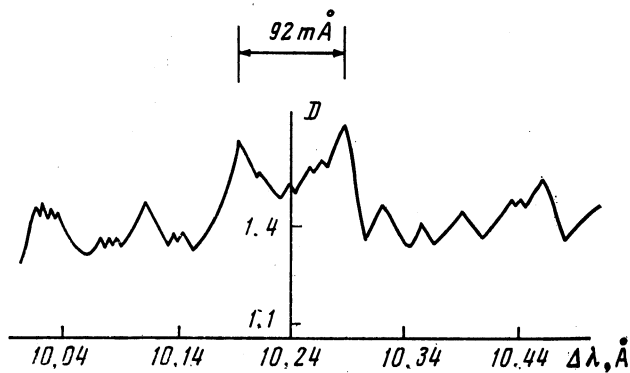


FIG. 6. Profile of the Ly_{β} line of Ne x recorded in experiment No. 4.

trons increased considerably the entropy of the DT gas and of the shell, which in the final analysis prevented the attainment of high plasma densities.

Calculations carried out using the SND program indicated that a reduction in the aspect ratio $R_0/\Delta R$, i.e., adoption of thicker shells ($\Delta R \approx 2-3 \mu\text{m}$), reduced the heating of the shell by hot electrons. This made it possible to reach DT gas densities in the range $\rho_f \gtrsim 1 \text{ g/cm}^3$ for targets and laser pulses with the following parameters: $2R_m \approx 80-120 \mu\text{m}$, $\Delta R \approx 2 \mu\text{m}$, $\rho_0 \approx (0.5-1) \times 10^{-2} \text{ g/cm}^3$, $E_L \approx 200-300 \text{ J}$, $\tau_L \approx 0.2-0.25 \text{ ns}$.

When the target and laser pulse parameters were close to those given above (experiment 4 in Table I), the spectrum of the hydrogen-like Ne was recorded (Fig. 5). The intensities of the lines did not rise much above the background, so that we were able to identify reliably only the Ly_{β} and Ly_{γ} lines. The intensity of the Ly_{α} line was comparable with the background radiation intensity.

The profile of the Ly_{β} line had a well-resolved two-component structure with the maxima of the components separated by $\Delta\lambda_{Ly_{\beta}} \approx 92 \pm 10 \text{ m}\text{\AA}$ (Fig. 6). Such a shift of the Ly_{β} line corresponded, for the selected chemical composition of the gas, to the DT gas density $\rho_f \approx 0.8-1.0 \text{ g/cm}^3$ and to the electron temperature $T_e \approx 0.3-0.4 \text{ keV}$. A gasdynamic calculation without using the SND program under the conditions of experiment No. 4 gave results in satisfactory agreement with experiments.

It should be pointed out that, in spite of the satisfactory description by these gasdynamic calculations of such experimental parameters as the absorbed energy, the fraction of the energy transferred to "fast" ions, the fraction of the energy carried by hard x rays, and the final density of the DT gas, there was a systematic excess (by a factor of $\sim 10^1-10^3$) of the calculated neutron yield N above the yield found experimentally. This was most likely due to the behavior of the temperature of the DT gas at the moment of focusing on the target, ignored in the calculations, and the resultant deviation of the real flow of the plasma from the assumed spherically symmetric geometry.

- ¹ S. B. Kormer, *Izv. Akad. Nauk SSSR Ser. Fiz.* **44**, 2002 (1980).
- ² A. I. Zaretskiĭ, G. A. Kirillov, S. B. Kormer, *et al.*, *Kvantovaya Elektron.* (Moscow) **10**, 756 (1983) [*Sov. J. Quantum Electron.* **13**, 468 (1983)].
- ³ A. I. Zaretskiĭ, G. A. Kirillov, S. B. Kormer, *et al.*, *Izv. Akad. Nauk SSSR Ser. Fiz.* **48**, 1611 (1984).
- ⁴ D. T. Attwood, D. W. Sweeney, J. M. Auerbach, and P. H. Y. Lee, *Phys. Rev. Lett.* **40**, 184 (1978).
- ⁵ V. P. Silin, *Usp. Fiz. Nauk* **145**, 225 (1985) [*Sov. Phys. Usp.* **28**, 136 (1985)].
- ⁶ J. S. Pearlman and M. K. Matzen, *Phys. Rev. Lett.* **39**, 140 (1977).
- ⁷ V. V. Aleksandrov, V. D. Vikharev, V. V. Gavrilov, *et al.*, *Plasma Diagnostics* [in Russian], Energoizdat, Moscow (1981), p. 61.
- ⁸ G. V. Dolgoleva, *Vopr. At. Nauki Tekh. Ser. Metod. Programmy Chisl. Resheniya Zadach Mat. Fiz. No. 2*, 29 (1983).
- ⁹ E. N. Avrorin, A. M. Zuev, Yu. N. Lazarev, *et al.*, *Vopr. At. Nauki Tekh. Ser. Metod. Programmy Chisl. Resheniya Zadach Mat. Fiz. No. 2*, 10 (1985).
- ¹⁰ B. Bezzerides, D. W. Forslund, and E. L. Lindman, *Phys. Fluids* **21**, 2179 (1978).
- ¹¹ D. W. Forslund, J. M. Kindel, and K. Lee, *Phys. Rev. Lett.* **39**, 284 (1977).
- ¹² Yu. N. Lazarev and N. P. Sitnikov, *Kvantovaya Elektron.* (Moscow) **10**, 2410 (1983) [*Sov. J. Quantum Electron.* **13**, 1570 (1983)].
- ¹³ V. L. Ginzburg, *Propagation of Electromagnetic Waves in Plasma*, North-Holland, Amsterdam (1961); Gordon and Breach, New York (1962); V. L. Ginzburg, *The Propagation of Electromagnetic Waves in Plasmas*, Pergamon Press, Oxford (1964); Addison-Wesley, Reading, Mass. (1964).
- ¹⁴ E. K. Storm, J. E. Swain, H. G. Ahlstrom, *et al.*, *J. Appl. Phys.* **49**, 959 (1978).
- ¹⁵ S. A. Bel'kov, A. I. Zaretskiĭ, G. A. Kirillov, *et al.*, *Vopr. At. Nauki Tekh. Ser. Termoyad. Sintez No. 2*, 28 (1987).
- ¹⁶ G. H. McCall, *Plasma Phys.* **25**, 237 (1983).

Translated by A. Tybulewicz